Applied Physics Research; Vol. 8, No. 1; 2016
ISSN 1916-9639 E-ISSN 1916-9647
Published by Canadian Center of Science and Education

Increasing Ultrasonic Array Data Acquisition Rate through the use of Kasami Codes and the Maximum Entropy Method

Eugeny Bazulin[1] & Andrey Bazulin[1]

[1] ECHO+ Ltd. Research and Production Center, str. Tvardovskogo, 8, Moscow, Russia

Correspondence: Eugeny Bazulin, ECHO+ Ltd. Research and Production Center, str. Tvardovskogo, 8, Moscow, Russia. E-mail: bazulin@echoplus.ru

Received: October 18, 2015 Accepted: October 30, 2015 Online Published: January 4, 2016

doi:10.5539/apr.v8n1p47 URL: http://dx.doi.org/10.5539/apr.v8n1p47

Abstract

We suggest using sets of pseudo-orthogonal code with antenna arrays working in Full Matrix Capture (FMC) mode, to increase the rate of data acquisition. This allows the use of signals comprised of phase-manipulated Kasami sequences, specifically developed for CMDA technology. The use of the Maximum Entropy Method (MEM) for decoding signals in lieu of matched filtration allows us to reduce noise level and increase time resolution in reflectors' image. Additionally, to reduce noise level by more than 6 dB we suggest the use of various Kasami sequences for each position of an antenna array. Numerical and model experiments demonstrate the efficacy of the proposed approach.

Keywords: antenna arrays, FMC, C-SAFT, TFM, CDMA, Kasami codes, Maximim Entropy Method (MEM).

1. Introduction

Currently, antenna rays are widely used in ultrasonic flaw detectors to visualize the internal structure of the targeted object: such as – most commonly – the internal technology of phased arrays (PA) (Olympus NDT., 2007), and the technology used by digital focus antenna (DFA) (Voronkov et al., 2011; Bazulin, Vopilkin, & Tikhonov, 2015). Bazulin (2013), which is dedicated to the comparison of PA and DFA, we conclude that DFA technology is more promising, therefore we consider it in more detail. In the first stage of DFA application echoes measured during the transmitting and receiving of all elements pair combinations within an antenna array (Kovalev et al., 1990). Bazulin (2001) refers DFA as the double scanning and Chatillon, Fidahoussen, and Calmon (2009) as Full Matrix Capture (FMC). Signal acquisition when antenna are working in both the double scanning mode and when moving is referred to as the «triple scanning mode». Bolotina et al. (2012) refers to this method as «migration arrays». In the second stage, image reconstruction is undertaken with the use of the combined SAFT method (C-SAFT) (Kovalev et al., 1990), which can be modified to account for multi-path ultrasonic testing of object with uneven borders (Bazulin, 2015). This method is also called the Total Focusing Method (TFM) (Chatillon, Fidahoussen, & Calmon, 2009). The possibility of coherently processing echo signals by C-SAFT for various antenna array positions allows one to obtain high quality images of reflectors that distinguish DFA from PA (Bazulin, 2013). However, the lack of acquisition when conducting double scanning is a large amount of measured data. By increasing the number of antenna array elements N_e data size increases quadratically. This leads to a decrease in the acquisition rate, as the transmission of echoes from the measuring unit to the image processing computer can be time consuming. This can be critical for a number of applications.

Another area where the reduction of acquisition rate is important is in medical diagnosis: to obtain high-quality images of moving internal organs. Arrays can consist of more than one hundred piezoelectric elements. With a PA comprised of 128 elements, with a pulse repetition frequency of 1 kHz and the beam focused at 300 angles (S-scan), obtaining an image takes approximately 0.3 seconds. This is comparable with the movement speed of internal organs and, as a result, obtaining high-quality images becomes difficult. Using echo acquisition in double-scanning mode reduces the time to 0.12 seconds, because the measurements are made in just 128 pulses (instead of 300 in PA mode) through a high-speed data transmission channel, but this still may not be sufficient for high-quality visualization of moving objects (Gutiérrez-Fernández, Jiménez, Martín-Arguedas, Ureña, & Hernández, 2013). Therefore, the tasks of increasing the speed and reducing the acquired data size are highly relevant for more efficient ultrasonic inspection.

2. Statement of the Problem

Let antenna array consists of N_e elements with δx element dimension and Δx distance between the elements centers. The procedure for registering echoes when double scanning is determined by the size of the switch matrix $\mathbf{C}$ with $N_e \times N_e$ size. If $\mathbf{C}_{nm} = 1$, this means that the radiating element has number n and receiving element has number m. Schematically, echoes are shown in Figure 1 at the left pane for four-element antenna array.

The set of echoes measured by all elements of the antenna array at the single radiation act of one element it called the **shot**, which are color coded in Figure 1 for various elements. Set of echoes for all shots called the **salvo**.

Since in this paper the acoustic aspect of the issue is minor, we therefore use the simplest model for the radiation and scattering of ultrasonic pulses. An antenna array consisting of N_e elements, without the wedge is placed on the surface of the inspected object, ultrasonic pulses are propagated through a homogeneous isotropic medium, the sound velocity is c, the reflection comes from the point scatterers with a refection coefficient $\varepsilon(\mathbf{r}_p)$ and located at the points N_p.

The field received with element m when radiating element is number n is written below

$$p_{nm}(t) = \int_{-\infty}^{\infty} p_{nm}^{\infty}(\tau) s(\tau - t) d\tau, \quad p_{nm}^{\infty}(t) = \sum_{p=1}^{N_p} \varepsilon(\mathbf{r}_p) \frac{\delta(t - (|\mathbf{r}_n - \mathbf{r}_p| + |\mathbf{r}_p - \mathbf{r}_m|)/c)}{|\mathbf{r}_n - \mathbf{r}_p||\mathbf{r}_p - \mathbf{r}_m|}, \tag{1}$$

where $\mathbf{r}_n$ and $\mathbf{r}_m$ are vectors for radiating and receiving elements positions; $s(t)$ – the system's reaction at δ -function impact. Figure 1 schematically shows four groups of echoes from one point scatterer for an array, consisting of four elements. For clarity, for each element is assigned a color that matches the color of the radiated pulses. If all elements of the switch matrix $\mathbf{C}$ are «1», $N_e \times N_e$ echoes will be measured with N_e shots. That is for the 32-elements antenna array, radiating 32 times, one need receive and store 1 024 echoes. The easiest way to reduce the amount of measured data is to fill with «1» only the upper or lower triangle of the matrix, which reduces about half the total size of the measured echoes, but does not reduce the acquisition time. One can randomly remove more than half cells from the matrix, but this approach will lead to an increase in noise in the reconstructed image.

Nonlinear methods of image reconstruction allow us to use about 10% of the full set of echoes (Bazulin, 2013), e.g. only 1 600 echoes for the 128 elements antenna array need to be measured, instead of 16 348 echoes. Such methods, however, are quite complex and require more time to reconstruct the image than when using the C-SAFT method.

From the perspective of multi-channel communications theory, double scan mode is similar to a situation where subscribers take turns sending a message that is subsequently received by all subscribers. The serial nature of the radiation probe pulse allows to answer the question: «Who is the source of the message?». Such a communication mode, when each pair of transmitter-receivers has the entire spectrum width, or most of it according to the selected time interval, is called Time-Division Multiple Access (TDMA) (Bernard, 2001). If all subscribers could send their messages simultaneously, and when receiving could filter all the messages and understand «Who sent the message?» – then this would drastically improve acquisition rate and data size.

To resolve this problem – when the channels have a common frequency band, but a different code modulation – Code Division Multiple Access (CDMA) technology has been developed (Bernard, 2001). For its implementation, each element of the antenna array must radiate its unique probe signal $s_n(t)$, while receiving echoes from all other elements in the antenna array. Schematically echo measurements in CDMA are shown in Figure 1 on the right. Measured echoes with (1) can be written as

$$p_m(t) = \sum_{n=1}^{N_e} p_{nm}(t), \quad p_{nm}(t) = \int_{-\infty}^{\infty} p_{nm}^{\infty}(\tau) s_n(\tau - t) d\tau \tag{2}$$

To apply the method of C-SAFT echoes $p_m(t)$ need to be decoded before subscriber m can select a $p_{nm}(t)$ message from the sender number n. Figure 1 shows the decoding procedure as the passage of a beam of light through a wedge.

Ideally, in the case of $N_e = 128$ this approach makes it possible to make a single shot instead of 128 measurements, and therefore reduce the number of echoes for the salvo from 16 348 to 128. It is clear that for this faster acquisition increase the time involved in echo decoding. Consequently the system may no longer generate an image with a frequency greater than 10 Hz. However, for expert post-processing with the automated inspection systems such performance restriction does not matter.

A similar approach is used in the high-speed inspection of rails when an antenna array simultaneously emits several probing pulses to form multiple ultrasonic beam incident angles (Alaix, 2006). However, dedicated publications do not mention the type of signal, not a decoding method.

Thus, the problem of increasing the acquisition rate may be formulated as: the need to find a set of signals $s_n(t)$ and decoding method, to recover signals $p_{nm}(t)$ according to formula (2) from the measured echo signals $p_m(t)$ and then reconstruct images by C-SAFT.

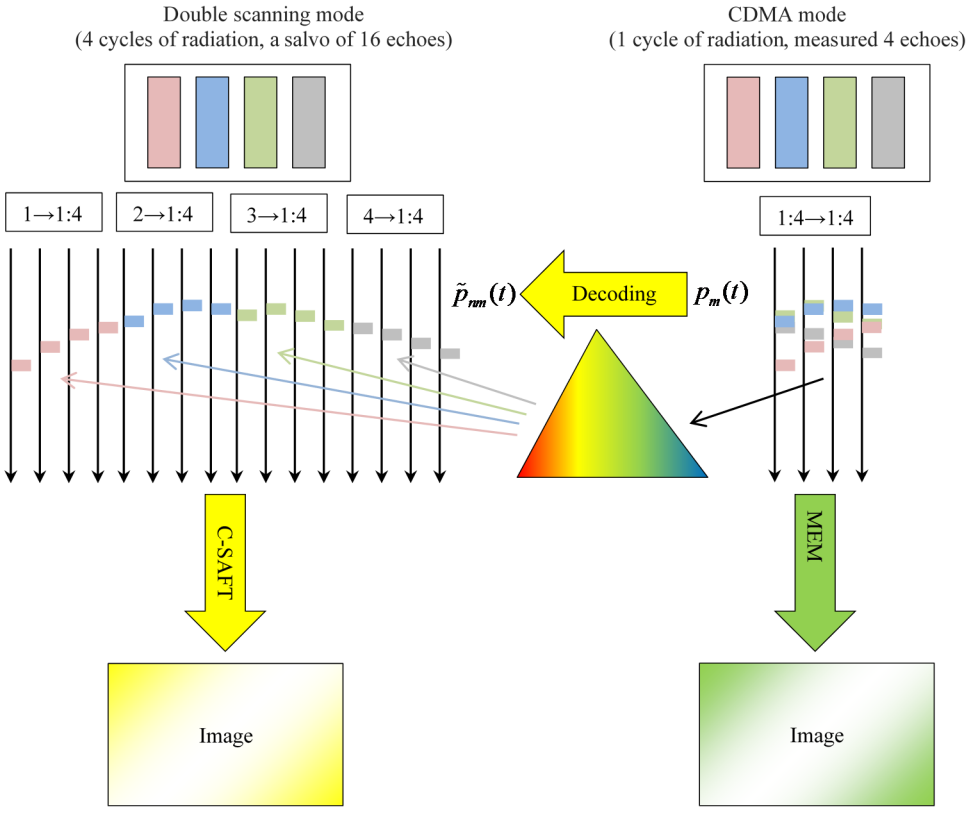

Figure 1. The principle of increasing the echoes acquisition rate

An important feature of the use of CDMA technology is that the simultaneous emission of all elements in the antenna array will result in the physical focus of the ultrasonic acoustic field along the axis of the wedge, which will reduce the size of the area in which one can restore the image of reflectors. One can reduce this effect with a defocused acoustic beam. For this purpose it is necessary to emit echoes with delays, rising to the edges of the antenna array, and take this into account in the subsequent calculation.

For effective decoding correlation function $R_{nm}(\tau)$ of encoding signals set $s_n(t)$ must have the following property

$$R_{nm}(\tau)=\int_{-\infty}^{\infty} s_n(t)s_m(t+\tau)dt=\begin{cases}\delta(\tau), n=m\\ 0, n\neq m\end{cases}, \tag{3}$$

where $n,m=1,2,...N_e$. A set of signals having the property (3) is called orthogonal. Several types of encoding signals sets have been developed, which are more or less close to the ideal set with properties (3) and are called «pseudoorthogonal». For the formation of the probing signals it was proposed (Gutiérrez-Fernández, Jiménez, Martín-Arguedas, Ureña, & Hernández, 2013) to use a phase-shift keyed with Kasami sequences (Kasami, 1966) signals with carrier frequency f_c. Kasami sequences belong to a class of pseudo-random signals and are generated by a shift register with length d and a feedback register of the same length. The number of codes in the Kasami set is $N_k=2^{d/2}$ and the length of the code is $N_c=2^d-1$, where d is an even number. That is, for a given value of the shift register and the feedback register is possible to generate one set of N_k pseudoorthogonal code signals $\{s_k(t)\}_{N_k}^s=\{s_1^s(t),s_2^s(t),...s_{N_k}^s(t)\}$. The index s points to a set of signals from one entire set of N_s dimensions that can

be generated for a predetermined length d of the shift register. In Perez et al. (2009) an algorithm is given for generating Kasami codes which have a correlation function with minimal side lobes of about $1/\sqrt{N_c}$.

Since generated probing signals are compound signals, the signal-to-noise ratio (SNR) is achieved by selecting the length of the code (Kasami, 1966). By increasing the length of the shift register from 6 to 8 bits, one can improve the SNR after deconvolution at 6 dB However, in non-destructive tests, it was found that the use of a signal with 63 periods essentially increases the dead zone size, not to mention Kasami codes with longer duration.

Figure 2 on the left shows the module of the correlation function $R_{nm}(\tau)$ $(n=5, m=1,2,...8)$ for $f_c=5$ MHz carrier frequency and the length of the shift register $d=6$. The initial value of the shift register is {1 1 1 0 1 1}, and feedback is given as {0 1 0 0 0 1}. Duration of probing signals is $w_t=12.6$ μs. The maximum value of the correlation function for defining the level of interference between channels was -12.5 dB, and its average level was -27.9 dB The width of the autocorrelation function at the 0.5 level was 0.3 μs. The correlation function $R_{nm}(\tau)$ had the same shape for the rest of the values n, that is, the set of code signals approximately satisfies the equation (3). Since the whole system has limited bandwidth, the actual phase-shift keyed signals $s_k(t)$ will differ from the ideal and the correlation function $R_{nm}(\tau)$ will have a higher level of inter-channel interference.

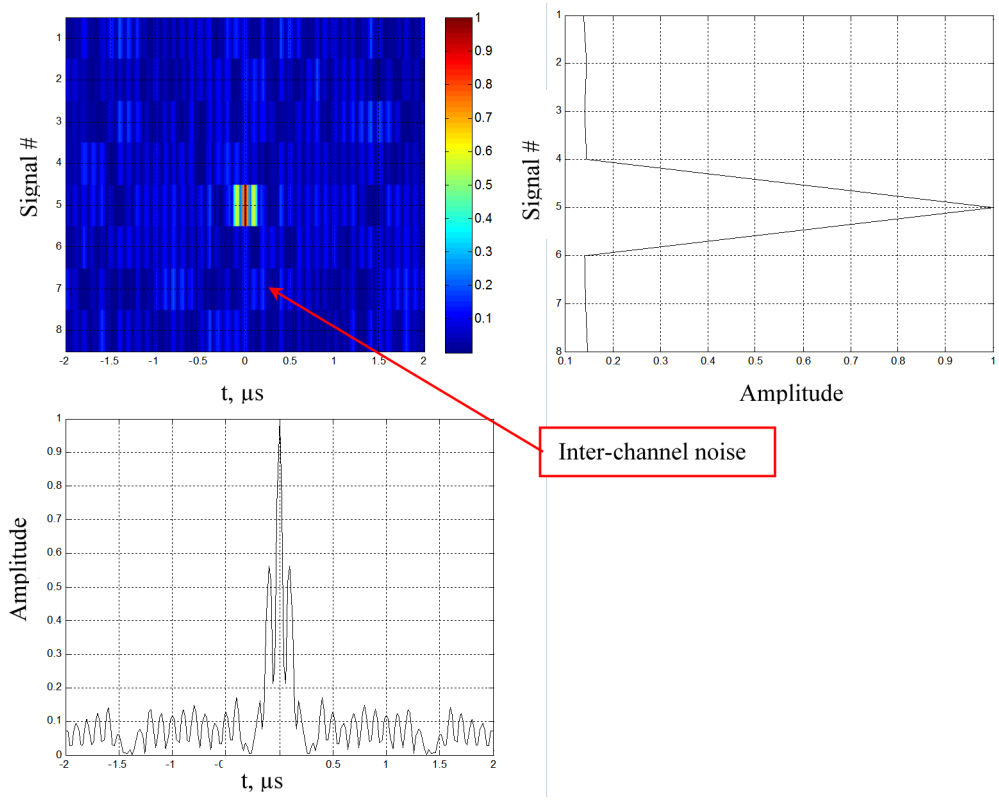

Figure 2. Example of the correlation function $R_{nm}(\tau)$ $(n=4, m=1,2,...8)$ for $N_c=63$

A set of code signals $\{s_k(t)\}_{N_k}^{s}$ was considered appropriate to use, if the level of inter-channel interference, i.e. the average of the correlation function module was less than –6 dB for $N_c=15$, less than –12 dB for $N_c=63$, less than –18 dB for $N_c=255$. The quantity of such sets N_d is shown in Table 1.

Table 1. Kasami codes properties

Register length	Code length N_c	Quantity of codes in set N_k	Quantity of code sets N_d	Inter-channel interference R_{nm}, dB
4	15	4	31	-6
6	63	8	185	-12
8	255	16	198	-18

It should be noted that the theory of CDMA technology also developed multiphase sequences which are also pseudoorthogonal, e.g. Frank sequence, Zadoff-Chu sequence (Frank, 1963; Chu, 1972). Zadoff-Chu sequence could be useful to accelerate the acquisition rate, as they have a number of advantages. For a sequence with length $N_c = 31$ it is possible to generate a set of $N_k = 29$ code sequences. There is no possibility to generate Kasami codes with $N_c = 31$ length.

Thus, the idea of acquisition rate increase is the simultaneous emission of special probing signals with all elements of the antenna array, or elements grouped into several subarrays. Reconstruction of reflectors images may occur due to the decoding of the summed echoes $p_m(t)$ to the $p_{nm}(t)$, as if they were measured in double scan mode. This branch in Figure 1 shown with yellow arrows and rectangle. The second branch, shown in Figure 1 with green arrow and rectangle, involves the image reconstruction with MEM from summed echoes $p_m(t)$.

2.1 Code Signals with Random Frequency

The code signal with a carrier frequency f_c belonging to one set have the following property

$$\sum_{k=1}^{N_k} s_k(t) = 0 \cdot \tag{4}$$

The echoes from reflectors located in the center of the main beam will arrive at the antenna array elements with delays that differ depending on the size of the antenna array and the distance of the elements from each other within the array.

The amplitude of the $p_m(t)$ echoes generated by the formula (2), due to the property (4), will decrease and, consequently, will depend on the distance between the reflector and the antenna array elements. If echoes are recorded from the reflector located on the acoustic axis of the antenna array, then the amplitude on the central elements of the antenna array, will be less than for the extreme elements due to the property (4).

To overcome this effect, one can use the following method: for each time code signal carrier frequency it is necessary to make the $f_c + \delta f$ random, where δf is the range of random f_c changes. It is enough to choose a range $\delta f > 0.1 f_c$ so that ratio (4) is no longer fulfilled. As a result, the correlation function $R_{nm}(\tau)$ of code echoes with random frequency will vary slightly from for constant (see Figure 2).

2.2. Image of Reconstruction by the C-SAFT Method

Since this paper uses several methods for reflectors image reconstruction, it is advisable to recall the principle of the C-SAFT method. The simplest variant of the C-SAFT enables to obtain the image of reflectors by the measured echoes according to formula

$$\hat{\varepsilon}(\mathbf{r}_i) = \sum_n \sum_m p_{nm}(t - t_n(\mathbf{r}_n, \mathbf{r}_i) - t_m(\mathbf{r}_m, \mathbf{r}_i)), \tag{5}$$

where $\mathbf{r}_i$ – the vector defining the position of the point of the region of interest (ROI), $\mathbf{r}_n$ and $\mathbf{r}_m$ – vectors defining the position of the emitting and receiving antenna array element, $t_n(\mathbf{r}_n, \mathbf{r}_i)$ and $t_m(\mathbf{r}_m, \mathbf{r}_i)$ – the travel time of the pulse from the point of emission or reception to the ROI point. Summation by the indices m and n takes place in accordance with the values of switching matrix **C**. To get more information about $\hat{\varepsilon}(\mathbf{r}_i)$ travel times functions can be calculated taking into account the multiple reflection of the pulse from the uneven surfaces of the inspected object and taking into account the effect of wave type transformation.

3. The Signals Decoding

After selecting a set of code signals $\{s_k(t)\}_{N_k}$ one needs to reconstruct the $p_{nm}(t)$ signals from measured $p_m(t)$ signals. If we use the analogy of color shown in Figure 1, the proper decoding allows us to select $p_{nm}(t)$ signals «painted» in only one color from the $p_m(t)$ source set. Given the fact that the pulses with «different colors» may be very close to each other, the decoding algorithm has to provide a precise time resolution.

The efficiency of the echo signals decoding algorithms depends on the type of reflectors and their number, since this influences how close echoes will be located to each other. That is the quality of the decoding echoes from one point of the reflector can be rather high (Bazulin, 2015), but for the processing of echoes from many reflectors, the reconstructed image can have unacceptably high levels of inter-channel interference.

3.1 Decoding using Matched Filtering

A common method for decoding a compression of compound $p_m(t)$ signals involves using the matched filter with the code signal $s_n(t)$. Given that the matched filtering in the time domain is equivalent to convolution (Bernard, 2001), the decoding operation can be written as

$$\tilde{p}_{nm}(t) = \int_{-\infty}^{\infty} p_m(\tau) s_n(\tau - t) d\tau . \quad (6)$$

This algorithm has a high speed of operation and allows one to reconstruct images at a frequency greater than 10 Hz, but it is not possible to get a low level of inter-channel interference and achieve the effect of super-resolution.

3.2 The Decoding using Maximum Entropy Method

A more sophisticated method of simple signals or compound signals deconvolution is based on the of maximum entropy method (MEM) (A. E. Bazulin & E. G. Bazulin, 2009). The convolution operation in equation (2) can be written in matrix form as:

$$s = Gs^{\infty} + n , \quad (7)$$

where the s – column vector with the measured echo N_t samples, G circulant matrix with $N_t \times N_t$ size, with rows built from code signals $s_n\{t\}$, s^{∞} – undistorted function that one want to restore, n – column vector of measurements noise. The braces in formulas indicate that the function is represented in a discrete form at the N_t time point.

The task of the deconvolution is to restore the s^{∞} by the measured signal $s_n(t)$, taking into account the $s_n\{t\}$. The problem (7) is ill-posed and Tikhonov and Arsenin (1986) developed a method of regularization, justifying the replacement problem in the form (7) for the optimization problem which is resistant to small changes in the input data s

$$\hat{s}_{\alpha} = \arg\min_{\hat{s} \in R^{N_t}} \left(\chi^2(\hat{s}\{t\}) + \alpha \Omega(\hat{s}\{t\}) \right), \quad (8)$$

where $\chi^2(\hat{s}\{t\}) = \left\| \hat{s}\{t\} - s\{t\} \right\|$ – squared residual in the R^{N_t} metric, $\Omega(\hat{s}\{t\})$ – stabilizing functional, α – Lagrange multiplier (regularization parameter). Estimation of the measured signal comes from the convolution $\hat{s}\{t\} = \hat{s}^{\infty}\{t\} \otimes s_n\{t\}$, where $\hat{s}^{\infty}\{t\}$ is estimation of the desired signal for a system with an infinite bandwidth, $s_n\{t\}$ – coded signal of the n th antenna array element.

The reason for using the stabilizing functional is to take into account *a priori* information about the properties of solutions and thereby narrow the search for solutions in solving of ill-posed problems. The cross-entropy of $\hat{s}$ (Kullback, 1968) can be used as the stabilizing functionality and (8) could be rewritten as

$$\hat{s}_{\alpha} = \arg\min_{\hat{s} \in R^{N_t}} \left(\chi^2(\hat{s}) - \alpha H(\hat{s}) \right), \quad H(\hat{s}) = -\sum_{i=1}^{N_t} \hat{s}_i \ln \frac{\hat{s}_i}{m_i}, \quad (9)$$

where m_i is an *a priori* model or solution s estimate. In the simplest case, a constant value $m_i = \mu$ can be used. In Maisinger, Hobson, and Lasenby (2003) the cross-entropy of oscillating function was calculated according to formula

$$\begin{aligned} z_i &= \sqrt{\hat{s}_i^{\,2} - 4\mu^2}, \\ H(\hat{s}) &= -\sum_{i=1}^{N_t} \left(z_i - 2\mu - \hat{s}_i \ln \frac{z_i + \hat{s}_i}{2\mu} \right), \end{aligned} \quad (10)$$

where it is recommended to take μ equal to 0.01 of the average value of the signal s. For an effective search of the minimum for functions of several variables by the second order methods the gradient and the Hessian of the expression (9) can be expressed as follows

$$\frac{\partial H(\hat{s})}{\partial \hat{s}_i} = -\ln\left(\frac{z_i + \hat{s}_i}{2\mu} \right), \quad \frac{\partial^2 H(\hat{s})}{\partial \left(\hat{s}_i\right)^2} = -\frac{1}{z_i} . \quad (11)$$

In formula (11) Hessian has the form of a diagonal matrix, this can accelerate the work of optimizing algorithms and reduce the requirements for the amount of RAM.

Thus, if the $s(t) = p_m(t)$ signal is a sum of the signals which are proportional to the code signal in accordance with formula (2), one can restore the $p_{nm}(t)$ signal by deconvolution of the measured $p_m(t)$ echoes according to formula (9) with the calculation of the entropy, its gradient and Hessian by formulas (10) and (11). The matrix G should be built with use of the code signal $s_n(t)$. Such a decoding method leads to the reconstruction of the signal estimate $\hat{p}_{nm}(t) \approx p_{nm}^{\infty}(t)$ with super-resolution.

3.3 Additional Techniques to Improve the SNR

3.3.1 Using of Multiple Kasami Code Sets for One Antenna Array

For a Kasami code sequence with code length $N_c = 63$ a set consists of eight signals ($N_k = 8$). Therefore, an antenna array of 32 elements ($N_e = 32$) could be divided down into four subarrays ($N_s = 4$), each of which consists of 8 elements.

For the full salvo measurement in CDMA mode it is necessary to carry out 16 cycles of measurements $N_{tr} = N_s^2$: radiating with the first subarray and receiving by the first subarray, radiating with the first subarray and receiving by the second subarray and so on until the fourth subarray radiates and receives on its own.

For each subarray measurement cycle one can use the same set of code signals $\{s_k(t)\}_{N_k}$. However, to reduce the level of inter-channel noise, one can use the following technique – use a different set of Kasami codes for each measurement cycle.

$$\left\{\{s_k(t)\}_{N_k}^{tr}\right\}_{N_{tr}} = \left\{\{s_k(t)\}_{N_k}^{1}, \{s_k(t)\}_{N_k}^{2}, \ldots \{s_k(t)\}_{N_k}^{N_{tr}}\right\}, \quad tr = 1,2,\ldots N_{tr}. \tag{12}$$

Since each set of correlation functions away from the main lobe has the form shown on Figure 2, it is natural to expect a decrease in the level of inter-channel interference at $\sqrt{N_{tr}}$ due to the fact that noise will not add coherently. This approach is more effective, when more elements N_e in an antenna array are used and a larger the number N_{tr} of sets of encoding signals used.

Antenna array can be divided into subarrays in several ways. Figure 3 (top) shows the case of the creation of four compact subarrays for $N_e = 32$, and Figure 3 (below) shows the creation of four sparse subarrays. There is also a variant where subarrays are created with a random selection of antenna array elements.

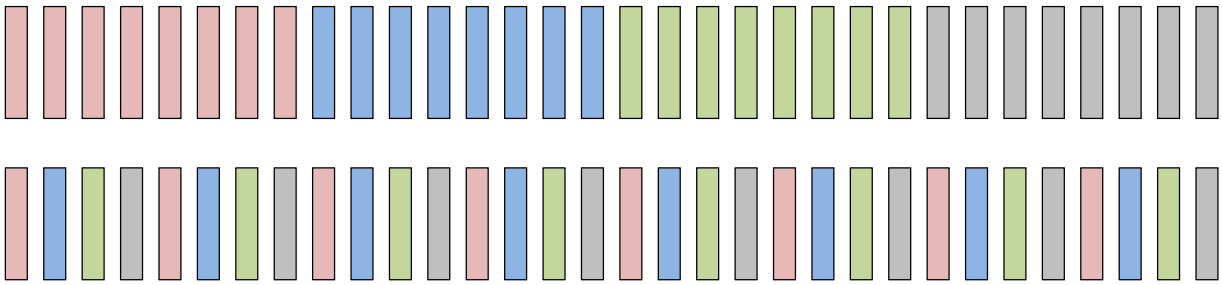

Figure 3. Two versions for the splitting of the antenna array with $N_e = 32$ at the subarrays. The elements of each subarray are marked with a different color

For Kasami code sequence with code length $N_c = 15$ set consists of four signals ($N_k = 4$). Therefore, an antenna array of 32 elements ($N_e = 32$) could be divided down into eight subarrays. For this case $N_{tr} = 64$ and the acquisition time in CDMA mode could be decreased only by half when compared with to double scan mode.

3.3.2 Using Multiple Kasami Code Sets for Different Antenna Array Positions

One can increase the spatial aperture of the antenna array when echoes are measured at multiple antenna array spatial positions N_w and the final image is formed by the coherent summation of N_w partial images (Bazulin, Vopilkin, & Tikhonov, 2015) reconstructed for each position of the antenna array. In this case, the level of inter-channel noise can be further reduced through a further generalization of the Section 2.4.1 approach, i.e. to use a different set of code signals with N_{tr} length for each position of the antenna array

$$\left\{\left\{\{s_k(t)\}_{N_k}^{tr}\right\}_{N_{tr}}^{w}\right\}_{N_w} = \left\{\left\{\{s_k(t)\}_{N_k}^{tr}\right\}_{N_{tr}}^{1}, \left\{\{s_k(t)\}_{N_k}^{tr}\right\}_{N_{tr}}^{2}, \ldots \left\{\{s_k(t)\}_{N_k}^{tr}\right\}_{N_{tr}}^{N_w}\right\}, \quad w = 1,2,\ldots N_w. \tag{13}$$

When using such an approach it is natural to expect a further reduction of the noise level in the final image at $\sqrt{N_w}$ with the coherent summation of N_w partial images. For the 32 element antenna array and $N_c = 63$ the number of positions N_w for which one can use a different set of code combinations is $N_w = N_d / N_{tr} \approx 11$. For the case when $N_c = 15$, the $N_w \approx 1$ and this technique is not available.

4. Image Reconstruction without Intermediate Signals Decoding

Section 2 described the methods that allow one to obtain $\hat{p}_{nm}(t)$ echoes as if measured in double scan mode, and how to undertake image reconstruction by the C-SAFT method. In Bazulin (2013, 2014) MEM was proposed as a way to reconstruct reflectors images from the echoes measured during double or triple scanning using sparse switching matrix $\mathbf{C}$. Such an approach allows the reconstruction of the image $\varepsilon(\mathbf{r}_i)$ with high resolution and low noise, using about 10% of the full set of echoes.

Let the solution of the direct problem, i.e. the calculation of the scattered field $p(\mathbf{r}_r,t)$ by present $q(\mathbf{r}_t,t)$ and $\varepsilon(\mathbf{r})$ can be written as follows:

$$p(\mathbf{r}_r,t)=P\left(\varepsilon(\mathbf{r}),q(\mathbf{r}_t,t)\right). \tag{14}$$

If the direct problem is linear or could be linearized, then formula (14) can be written in the form of a matrix similar to formula (7)

$$p=G\varepsilon+n, \tag{15}$$

where matrix G describes the propagation of ultrasonic waves from the source point $\mathbf{r}_t$ to the reflector and to the point of reception point $\mathbf{r}_r$, vector n – measurements noise. Since the G matrix is ill-conditioned, then, as in Section 3.2 for the solution (15) one can apply a regularization by formula (9). From the perspective of mathematics there is no difference between formulas (7) and (15); physically there is principle difference, since these formulas describe different physical processes.

If one uses as the source data not $p_{nm}(t)$ but CDMA mode signals $p_m(t)$ MEM also allows to receive images with super-resolution and low noise. The image reconstruction algorithm is similar to formula (9) and can be written as follows

$$\hat{\varepsilon}=\arg\min_{\hat{s}\in R^{N_xN_z}}\left(\chi^2(\hat{\varepsilon})-\alpha H(\hat{\varepsilon})\right),\quad H(\hat{\varepsilon})=-\sum_{i=1}^{N_xN_z}\hat{\varepsilon}_i\ln\frac{\hat{\varepsilon}_i}{m_i}, \tag{16}$$

where $\chi^2(\hat{\varepsilon})=\sum_{m=1}^{\cdot\cdot\cdot}\left\|\hat{p}_m(t;\hat{\varepsilon})-p_m(t)\right\|$ is the squared residual in the metric $R^{N_xN_z}$ determined by size amount of ROI, $\hat{p}_m(t;\hat{\varepsilon})$ is estimate of echoes from a given $\hat{\varepsilon}$. This reconstruction option in shown on the right hand of Figure 1 with a green arrow and square. To solve equation (16) or (9), one can use the second order iterative procedures to find the minimum of many variables function. Gradient and Hessian are calculated by formulas (10) and (11). To distinguish the method used for the echoes deconvolution with MEM (see Section 3.2), the method considered in this Section will be called as MEM+C-SAFT.

The main methodological problem of MEM+C-SAFT practical application is the selection of regularization parameter α and background amplitude μ. There are exact and empirical methods to choose: the α–residual method, the method of cross-checking, L-curve method and others. However, some methods are iterative and therefore require substantial computing resources, and others need more information, such as the value of the noise dispersion, which may not be estimated with sufficient accuracy. In many practical papers devoted to the application of the MEM, the problem (16) is solved for a variety of regularization parameters α, and one to choose the best solution according to some criteria. In this paper we chose $\hat{\varepsilon}_\alpha$ with best focusing (e.g. with minimal size of point-type reflector image). The matrix form of equation (15) makes possible to estimate the $\hat{\varepsilon}$ function similar to the correlation formula as

$$\hat{\varepsilon}=G^T p, \tag{17}$$

where the symbol *T* denotes the transposed matrix.

4.1 The Required Computing Resources

To obtain an 200×200 pixels image a matrix G has size 40 000×40 000. If one works with doubles, then one need 128 GB of RAM. The times for some operations for prectical MEM+C-SAFT calculation on PC with 12 processors are shown in the Table 2.

If one uses the single-precision or an integer data format, then the memory requirements can be reduced by ten times. If one will optimize the software implementation of the MEM+C-SAFT algorithm, it can be expected to speed up ten times and ten times reduce required RAM. Besides the rapid development of computer technology reduces the technical problems of the MEM+C-SAFT implementation.

Table 2. The times for some operations for MEM+C-SAFT

Stage	Time	Comment
G matrix calculation	≈70 sec	Time could be decreased up to two orders of magnitude due to the use of parallelizing calculations
G matrix transposition	≈10 sec	
Hessian calculation	≈2500 sec	The most time consuming operation to accelerate, as should be done about 64×10^{12} operations
Image calculation with formula (17)	≈2 sec	
Minimization of function (16) (MEM+C-SAFT)	Minutes	Time depends on α and μ values

5. Numerical Experiments

To test the proposed algorithms simple echo calculations were performed according to (1) from the point scatterers and antenna array without a wedge. The sound velocity in the object was assumed to be 5.9 mm/ s. The sampling frequency is 50 MHz

Ten point reflectors with different reflection coefficients were selected as the test objects, the parameters of which are given in the Table 3. A scheme of the numerical experiment is shown in Figure 4.

Table 3. Parameters of point reflectors

Reflector number	1	2	3	4	5	6	7	8	9	10
x, mm	0	0	0	0	0	0	0	0	0	0
z, mm	30	31	32	33	34	35	36	37	38	39
Reflection coefficient $\varepsilon(\mathbf{r}_i)$	0.1	1.0	0.2	0.9	0.3	0.8	0.4	0.7	0.5	0.6

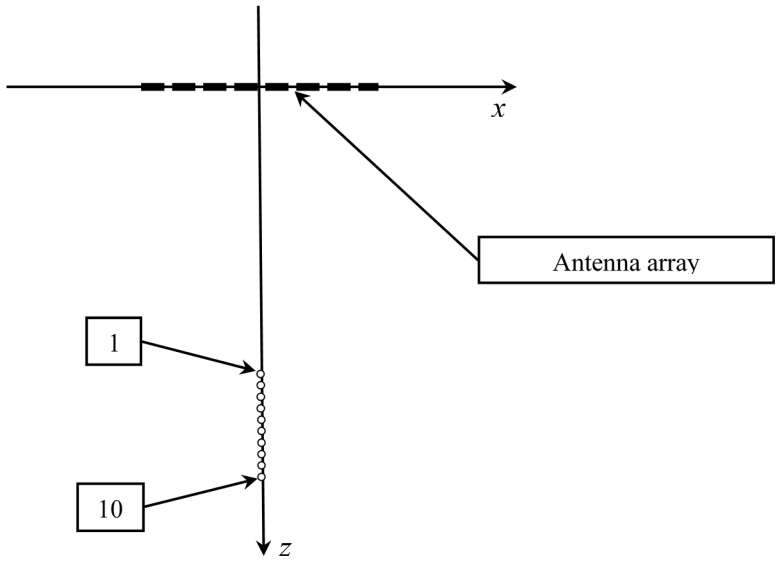

Figure 4. Scheme of the numerical experiment

Figure 5 (left hand) shows the ideal resulting image of the ten point reflectors when indication size is one pixel, and the image is restored by C-SAFT from echoes measured in double scanning mode with an antenna array of 16 elements with a pitch 1.0 mm, for the full switching matrix $\mathbf{C}$ according to formula (1) (right hand). The probe pulse was a radio signal with 5 MHz carrier frequency and a Gaussian envelope with three periods length. C-SAFT images allow the detection of all reflectors including the first, which has the smallest reflection coefficient.

Moreover indications amplitudes are within 2% identical range of the specified $\varepsilon(\mathbf{r}_i)$ in Table 2. Longitudinal and front resolutions correspond to the length of the probe pulse and the aperture of the antenna array. The level of background noise along the acoustic axis of the antenna array is less than -40 dB.

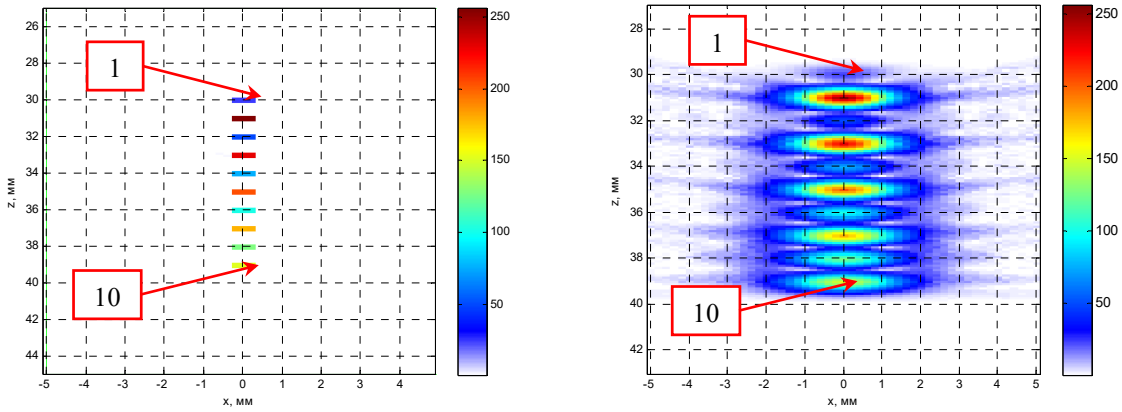

Figure 5. On the left an ideal image of the test object, on the right C-SAFT restored image for echoes measured in double scan mode

5.1 Kasami Codes with Length 63

5.1.1 Antenna Array with 16 Elements and 1.0 mm Pitch

Since for $d=6$ the number of signals in one set is $N_k=8$, an antenna array of 16 elements can be divided into two subarrays. The first corresponds to the array elements 1 to 8, and the second – from 9 to 16 (similar to Figure 3, top). Therefore it was necessary to carry out four measurements for subarrays ($N_{tr}=4$), that is, instead of the 256 echoes for 16 cycles of radiation in double scan method we measured 32 echoes for 4 cycles of radiation. In comparison with the double scan this means a fourfold increase in acquisition rate and an eightfold decrease in memory capacity required for recording the echo signals and transmitting them over the communication channel.

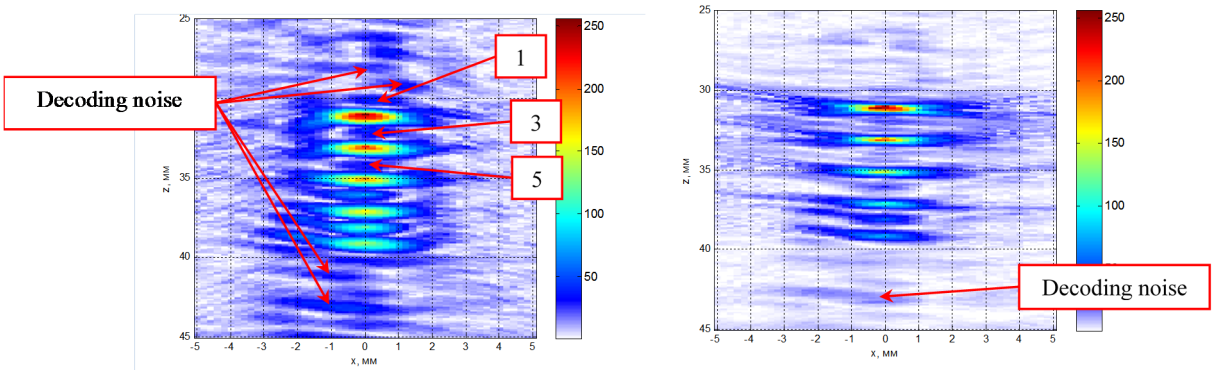

Figure 6. C-SAFT image of the test object, when echoes are decoded with matched filtering (left) and by the MEM+C-SAFT (right). 16 elements array was not divided to subarrays

Figure 6 (left) shows the result of restoring a C-SAFT image decoding using matched filtering according to formula (6) in the frequency range [0.5, 8.5] MHz. For each of the four measurement sublattices ($N_{tr}=4$) a specific set of Kasami codes was used in accordance with (12). The maximum amplitude of inter-channel noise was –16 dB, making the reconstructed image of little practical use, since the images from reflectors # 1, 3 and 5 is extremely difficult to identify. If decoding is performed with MME according to (9), ($\alpha=5$, $\mu=10^{-4}$), the maximum value of the interchannel noise in an image reduced to minus 24 dB (Figure 6, right), the beam resolution decreased twice. However, the amplitude of the reflectors # 1, 3 and 5 are still extremely difficult to identify. For this reason, the image is still not high-quality.

Two Kasami codes sets can be combined into one set. This will allow us to increase the acquisition rate for a 16 element array, not four times but sixteen times. However, this will lead to an increase in inter-channel noise, because, using the terminology of the theory of communication, the communication channel will be used not by eight subscribers at the same time, but by sixteen.

The image may be reconstructed by the MEM+C-SAFT with formula (16) without decoding echoes. Figure 7 (right) shows image reconstruction with correlation method (Gutiérrez-Fernández, Jiménez, Martín-Arguedas, Ureña, & Hernández, 2013), and on the right by the MEM+C-SAFT ($\alpha = 0.1$, $\mu = 10^{-4}$). The image reconstructed by the correlation method, is quite close to that shown in Figure 6 on the left and has a high noise level that does not allow us to confidently detect reflectors # 1, 3 and 5. However, the image reconstructed by MEM+C-SAFT, is almost identical with the ideal, shown in Figure 5 (left). It can be considered a high image quality, since the noise level is less than minus 60 dB, and the beam and front resolutions increased more than fourfold compared to the image reconstructed by the correlation method. The amplitudes of reflectors differ from the ideal values of less than 1%. Of course, such an increase in image quality is due to the absence of noise, including the model noise, allowing the estimation of echoes in formula (16) to be almost the same as echoes when «measured experimentally». Unfortunately, the MEM+C-SAFT does not allow us to build real time images without conducting calculations on a supercomputer.

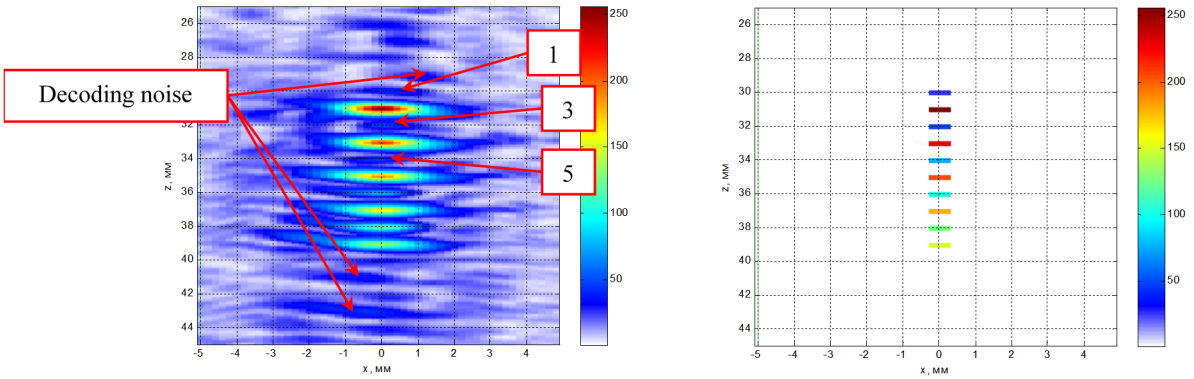

Figure 7. The image reconstructed with correlation method (left) and by MEM+C-SAFT (right). 16 elements array

Two Kasami codes sets, each of $N_k = 8$ length can be combined and the resulting MEM+C-SAFT, still gives an ideal image similar to Figure 7 (right). Moreover, the measurement of the echo is takes sixteen times less time in comparison with the double scanning method, and the size of the measured echoes $p_m(t)$ is sixteen times less than $p_{nm}(t)$.

5.1.2 Antenna array with 32 Elements and 0.5 mm Pitch

Using a 32 element antenna array with 0.5 mm pitch should improve the image quality, if one splits the antenna array into four subarrays, and for each radiating-receiving pair chooses a code set (see Section 3.3.1). Such an approach will allow us to measure not 1 024 echoes for 32 cycles, but only 128 echoes per $N_{tr} = 16$ cycles, that is, the acquisition rate is only 50% faster, but the amount of memory required to store the echo is reduced eight times.

The antenna array has been split into four subarrays (see Figure 3, top). Figure 8 (left) shows the result of a C-SAFT image reconstruction from echoes decoded using matched filtering according to formula (6) in the frequency range [0.5, 8.5] MHz The image is sufficiently close to the image shown in Figure 5 (right). Figure 8 shows (right) shows an image reconstructed from echoes decoded with MEM (8) ($\alpha = 5$, $\mu = 10^{-4}$). Reflector images in Figure 8 have a noise level of approximately 6 dB less than the same images in Figure 6. It is still difficult to identify reflectors # 1 and 3.

If the antenna array is divided into four sparse subarrays (see. Figure 3, bottom), the images which are reconstructed with C-SAFT from echoes decoded with matched filter and MEM, are shown in Figure 9. It can be seen that the noise level is noticeably smaller than in Figure 8.

If the antenna array is divided into four sparse subarrays (see Figure 3, bottom), the images reconstructed with C-SAFT from echoes decoded with matched filter and MEM, are shown at Figure. 9. It can be seen that the noise level is noticeably smaller than in figure. 8. Comparison of images at Figure 8 and Figure 9 allows making some

conclusions. First, it is better to split an antenna array into subarrays with as big aperture for each as possible. One variant is shown at Figure 3 (bottom). Secondly, echoes deconvolution with MEM on the one hand allows to reduce the inter-channel noise and improve the resolution, but on the other hand there are some amplitude distortions. This leads to the fact that it is difficult to detect reflectors # 1 and 3 at Figure 9 (right).

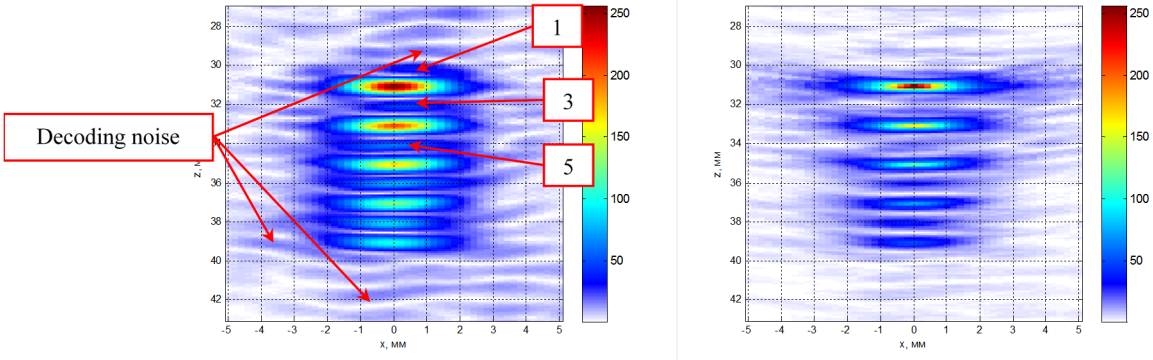

Figure 8. C-SAFT image of the test object, when echoes decoded with matched filtering (left) and by the MEM (right). 32 elements array divided in four subarrays

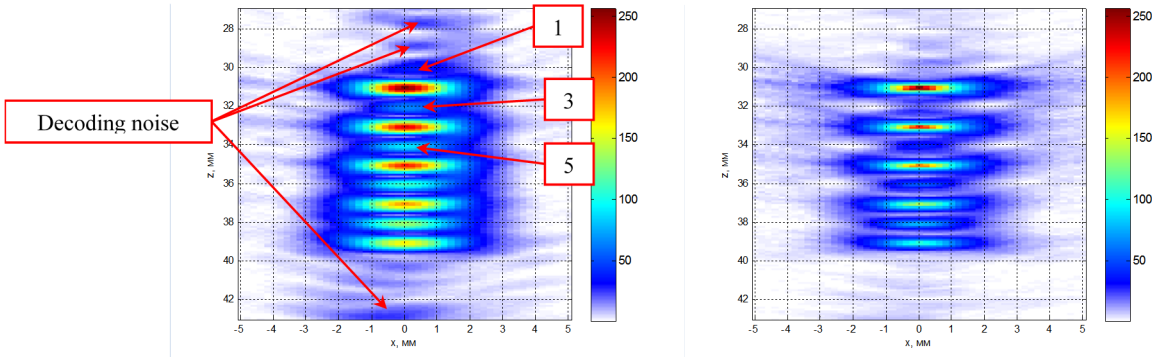

Figure 9. C-SAFT image of the test object, when echoes decoded with matched filtering (left) and by the MEM (right). 32 elements array was divided in four sparse subarrays

If, in order to maximize the acquisition rate, an antenna array is not split and uses a set of 32 code signals, the reconstructed images are shown in Figure 10. The noise level is more than in images reconstructed using an antenna array with 16 elements (Figure 6).

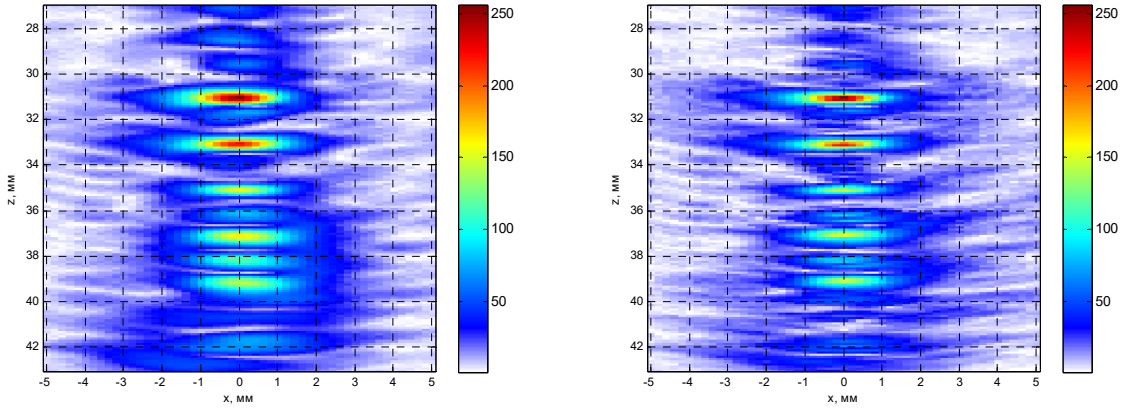

Figure 10. C-SAFT image of the test object, when echoes decoded with matched filtering (left) and by the MEM (right). 32 elements array not divided into four sparse subarrays

An image reconstructed with MEM+C-SAFT by formula (16) without decoding the echoes, is again indistinguishable from the ideal image in Figure 7 (right).

5.2 Kasami Codes with Length 15

Since for $d=4$ the number of signals in one set $N_k=4$, and the code length $N_c=15$ – the 16 elements antenna array was split into four subarrays ($\{\{s_k(t)\}_{N_k}^{tr}\}_{N_{tr}}$, $N_{tr}=16$). So we had to make sixteen «measurements» with subarrays, i. e. instead of 256 echoes for 16 radiation cycles we «measured» 64 echoes for the same 16 radiation cycles. That is, this approach has allowed reduce fourfold the amount of memory required to record the echoes and transmit it over the communication channel.

Figure 11 (left) shows the result of a C-SAFT image reconstruction from echoes decoded using matched filtering according to formula (6) in the frequency range [0.5, 8.5] MHz In comparison to Figure 6 (left) the maximum noise amplitude decreased to –18 dB, and it is possible to detect reflector # 5. However, the noise in the transverse direction was increased significantly, which would not allow us to detect a reflector with a small amplitude, offset from the axis of the antenna array. Image reconstructed from echoes decoded with MME ($\alpha=5$, $\mu=10^{-4}$) has a halved longitudinal resolution. We note that images in Figure 11 have no higher quality when compared with Figure 5 (right).

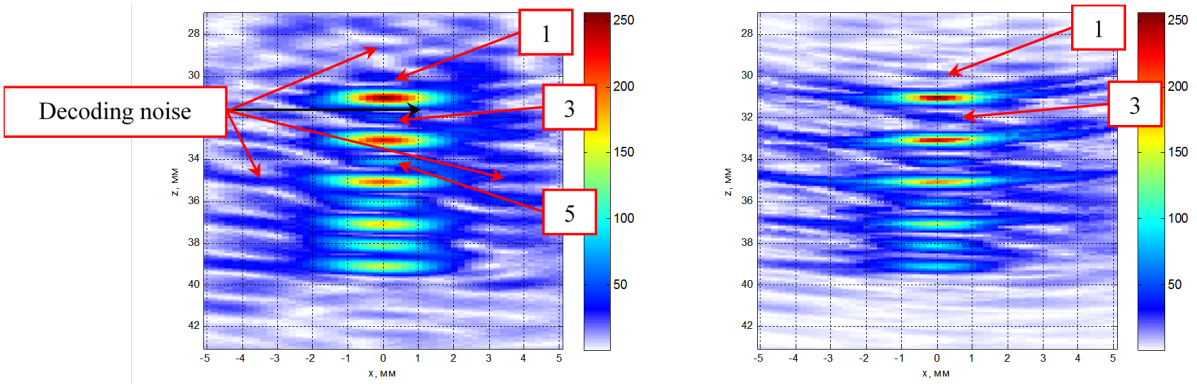

Figure 11. C-SAFT image of the test object, when echoes decoded with matched filtering (left) and by the MEM (right). 16 elements array divided in four subarrays. The length of the Kasami codes is 15

If we combine four Kasami codes in one set and increase acquisition rate by sixteen times, this leads to a significant drop in image quality (Figure 12), even in comparison with Figure 11.

An image reconstructed with MEM+C-SAFT by the formula (16) without decoding the echoes, is still indistinguishable from the ideal image in Figure 7 (right).

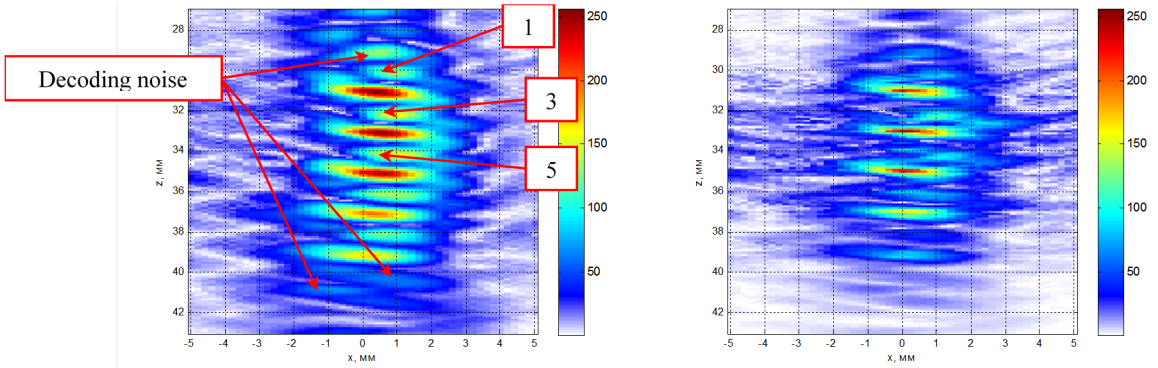

Figure 12. C-SAFT image of the test object, when echoes decoded with matched filtering (left) and by the MEM (right). 16 elements array without dividing to subarrays. The length of the Kasami codes is 15

6. Model Experiments

To carry out experiments one needs to have equipment that is capable of emitting code signals from each element. Currently, such equipment is being developed in SPC «ECHO+». However, the effectiveness of the proposed approach according to formula (16) can be demonstrated as follows. All echoes of shots in usual double scanning mode can be summated and this simulates data which could be obtained with simultaneous radiating and receiving from all array elements.

Figure 13 gives the sketch of a duralumin sample with side-drilled holes of a 0.5 mm diameter. The holes are located at a depth of 38 mm and the distance between the centers is 2 mm. 32 element antenna array were used with an operating frequency of 5 MHz and 0.8 mm pitch mounted on wedge of rexolite with a 35 degrees angle. Echoes were measured in four positions when moving in 9 mm steps from the starting point at -32 mm ($N_w = 4$). The antenna array and a wedge in the first and fourth positions are shown schematically in Figure 13.

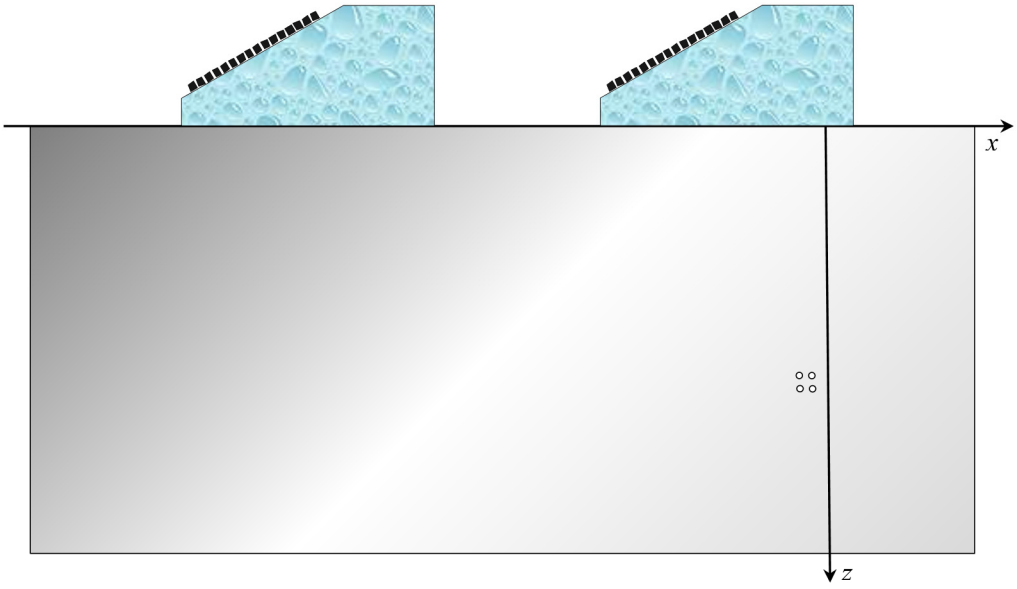

Figure 13. Test with side drilled holed

Figure 15 shows the result of image reconstruction with C-SAFT by all 4×1024 echoes $p_{nm}(t)$ in four antenna array positions. Black circles shows the real position of holes. The image does have a high resolution and there are false images related to the run round wave and rescattering between holes. So it is hard to determine reflectors types and quantity.

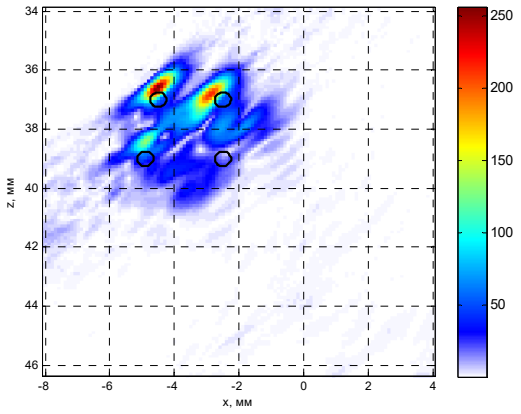

Figure 14. C-SAFT reconstructed image from all echoes in four array positions ($N_w = 4$)

It is possible to reconstruct image with MEM+C-SAFT (Bazulin, 2013; Maisinger, Hobson, & Lasenby, 2003) with just $p_{1m}(t)$ echoes set, i.e. using 4×32 echoes instead of 4×1024 echoes. Figure 15 (left) shows the result of image reconstruction by correlation method, and (right) by the MEM+C-SAFT ($\alpha = 20.0$, $\mu = 10^{-4}$). The image reconstructed by the correlation method by formula (17) has a frontal resolution of around 3 mm, and a side lobe level at -12 dB The image reconstructed by MEM+C-SAFT, can to be a high quality image because the noise level is less than -30 dB, and the longitudinal and frontal resolutions have more than doubled in comparison with the image reconstructed by the correlation method. Image reconstructed with MEM+C-SAFT clearly shows three holes and image of the fourth hole has a 12 dB lower amplitude due to the screening effect.

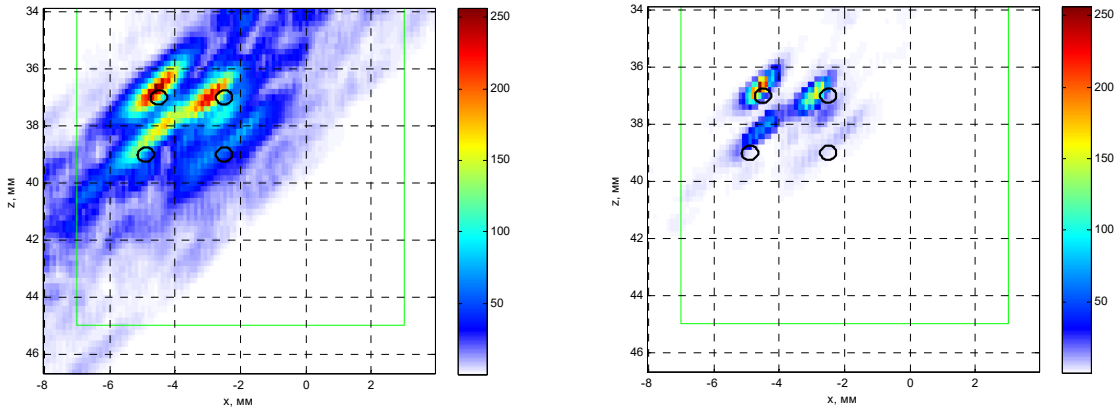

Figure 15. The image reconstructed by correlation method (left) and by MEM+C-SAFT (right) from single shot for each of four array positions

Figure 16 (left) shows the image reconstructed by the correlation method, and on (right) by MEM+C-SAFT with formula (16) ($\alpha = 2.5$, $\mu = 10^{-4}$) from summed 4×32 echoes $p_m(t)$. Shown in Figure 16 it is quite close to the image shown in Figure 15. Summed echoes $p_m(t)$, contains more information on the reflectors than just the first shot $p_{1m}(t)$, and generally their use in MEM+C-SAFT will be more effective.

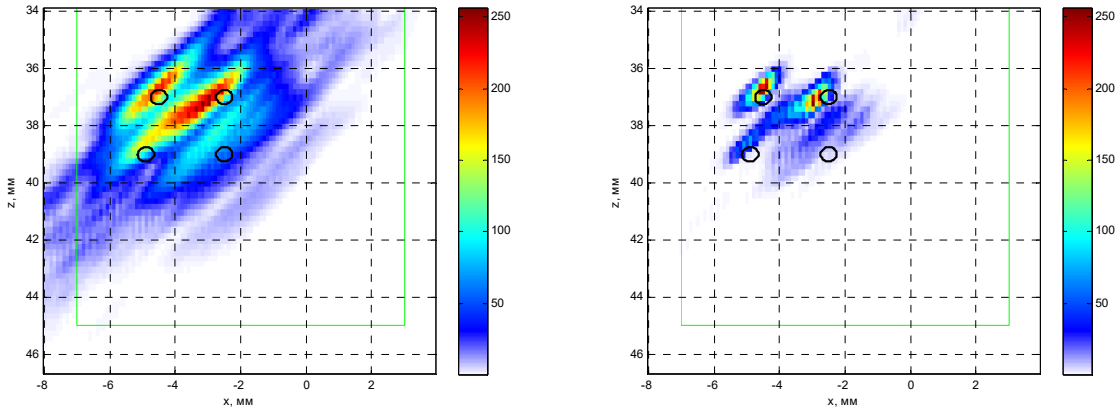

Figure 16. Image reconstructed by correlation method (left) and by MEM+C-SAFT (right). Echoes from each shot for each array position were summed before reconstruction

It should be noted that the use of compound signals generated using Kasami codes $\left\{\{s_k(t)\}_{N_k}^{tr}\right\}_{N_{\Sigma}}$ should further improve the quality of images reconstructed by MEM+C-SAFT, since the objective function will have a greater gradient in the neighbourhood of the global minimum.

7. Conclusions

(1) The use of CDMA technology has shown promise for code sequences based on Kasami codes. When the length of the shift register is $d=6$ for a 32 elements antenna array it can be increase the acquisition rate by eight times, and reduce the size of the measured echoes by sixteen times.

(2) The use of multiple sets of Kasami codes for different subarray combinations and antenna positions by formula (12) and (13), reduces the level of inter-channel noise, which allows the detection of small reflectors (Figure 9).

(3) Echoes decoding can be undertaken with matched filtering by formula (6) or MEM by formula (9), which gives more than 6 dB less noise, but distorts the amplitudes of reflections from reflectors with low reflection coefficient.

(4) The result of echo decoding and, therefore, the image quality strongly depends on the number of reflector; the more reflectors – the higher the level of inter-channel interference.

(5) It is better to choose the subarrays with maximum length (Figure 3, Figure 8 and Figure 9).

(6) In order to implement this approach, the flaw detector hardware must be able to emit compound signals.

(7) Image reconstruction by MEM+C-SAFT in numerical and model experiments by the formula (16) from echoes $p_m(t)$ allowed us to obtain almost perfect images (Figure 5, left and Figure 7, right). The acquisition time and memory required for storing echoes is N_e times less than for double scanning with switch matrix $\mathbf{C}_{nm}=1$. The result is perfect even for Kasami codes where length is $N_c=15$ without splitting array on subarrays. However, this approach does not allow for real time images reconstruction. It is also important to state that the application of formula (16) can be used for simple signals, rather than a set of pseudo-orthogonal signals. It does not require special equipment to emit compound signals.

(8) The proposed approach is promising for the inspection of thick-walled objects made of materials with high attenuation, because the use of compound signals increases the SNR and the such thickness would require the use of antenna arrays with many elements.

Acknowledgement

We are grateful to SPC «ECHO+» employee Alexander Butov for the comments made during the preparation of this paper.

SPC «ECHO+»

Bazulin Andrey, Bazulin Eugeny

2015 September 26th, 2015 December 24th

References

Alaix, R. (2006). *High speed rail testing with phased array probes*. Speno international, Geneva, Swaziland. Retrieved from http://www.uic.org/cdrom/2006/wcrr2006/pdf/242.pdf

Bazulin, A. E., & Bazulin, E. G. (2009). Deconvolution of complex echo signals by the maximum entropy method in ultrasonic nondestructive inspection. *Acoustical Physics*, *55*(6), 832-842.

Bazulin, E. G. (2001). Utilization of double scanning in ultrasonic testing to improve the quality of the scatterer images. *Acoustical Physics*, *47*(6), 649-653.

Bazulin, E. G. (2013). Comparison of systems for ultrasonic nondestructive testing using antenna arrays or phased antenna arrays. *Russ. J. Nondestr. Test., 7*, 404–423.

Bazulin, E. G. (2013). On the possibility of using the maximum entropy method in ultrasonic nondestructive testing for scatterer visualization from a set of echo signals. *Acoustical Physics*, *59*(2), 210-227.

Bazulin, E. G. (2014). Reconstructing the Deflector Images from the Ultrasonic Echo Signals by the Maximum Entropy Method. *Applied Physics Research*, *6*(6), 87-106. http://dx.doi.org/10.5539/APR.V6N6P87

Bazulin, E. G. (2015). Increasing the rate of recording ultrasonic echo signals in the double-scanning mode. *Russian Journal of Nondestructive Testing*, *51*(3), 151-165.

Bazulin, E. G. (2015). Reconstruction of reflector images using the C-SAFT method with account for the anisotropy of the material of the test object. *Russian Journal of Nondestructive Testing*, *51*(4), 217-226.

Bazulin, E. G., Vopilkin, A. Kh., & Tikhonov, D. S. (2015). Improved reliability of ultrasonic inspection. Part 1: Determine the type of discontinuity flaws during ultrasonic testing using antenna arrays. *Kontrol. Diagnostika, 8*, 7-22.

Bernard, S. (2001). Digital communications fundamentals and applications. *Prentice Hall, USA*.

Bolotina, I., Dennis, M., Mohr, F., Kröning, M., Reddy, K. M., & Zhantlessov, Y. (2012). 3D Ultrasonic Imaging by Cone Scans and Acoustic Antennas // *18th World Conference on Nondestructive Testing*. 16-20 April 2012, Durban, South Africa.

Chatillon, S., Fidahoussen, A., & Calmon, I. P. (2009). Time of flight inverse matching reconstruction of ultrasonic array data exploiting forwards models. *NDT in Canada 2009 National Conference*. Aug 25-27, 2009.

Chu, D. C. (1972). Polyphase codes with good periodic correlation properties. *IEEE Trans. Inform. Theory* (pp 531-532). July. 1972. http://dx.doi.org/10.1109/TIT.1972.1054840

Frank, R. L. (1963). Polyphase codes with good nonperiodic correlation properties. *IEEE Trans. Inform. Theory* (pp. 43-45). Jan. 1963. http://dx.doi.org/10.1109/TIT.1963.1057798

Gutiérrez-Fernández, C., Jiménez, A., Martín-Arguedas, C. J., Ureña, J., & Hernández, Á. (2013). A novel encoded excitation scheme in a phased array for the improving data acquisition rate. *Sensors*, *14*(1), 549-563.

Kasami, T. (1966). Weight Distribution Formula for Some Class of Cyclic Codes. *Tech. Report No. R-285, Univ. of Illinois. 1966. April*.

Kovalev, A. V., Kozlov, V. N., Samokrutov, A. A., Shevaldykin, V. G., & Yakovlev, N. N. (1990). Pulsed echo method in concrete testing. *Noise and spatial selection, Defektoskopiya*, (2), 29-41.

Kullback, S. (1968). *Information Theory and Statistics*. New York.

Maisinger, K., Hobson, M. P., & Lasenby, A. N. (2003). Maximum-entropy image reconstruction using wavelets. *Monthly Notices of the Royal Astronomical Society*, *3*, 1-21.

Olympus NDT. (2007). *Advances in Phased Array Ultrasonic Technology Applications*. Waltham, MA: Olympus NDT. Retrieved from http://www.olympus-ims.com/en/books/

Perez, M. C., Urena, J., Hernandez, A., Jimenez, A., Ruı, D., Alvarez, F. J., De Marziani, C. (2009). Performance comparison of different codes in an ultrasonic positioning system using DS-CDMA. *Proceedings of the IEEE International Symposium on Intelligent Signal Processing* (pp. 125–130). - WISP'09. Budapest. Hungary. 26–28 August. 2009.

Tikhonov, A. N., & Arsenin, V. Y. (1986). *On the solution of ill-posed problems* (3rd ed., revised). Moscow: Nauka. (in Russian)

Voronkov, V. A., Voronkov, I. V., Kozlov, V. N., Samokrutov, A. A., & Shevaldykin, V. G. (2011). Applicability of the antenna–array technology when solving problems of ultrasonic testing of hazardous industrial objects. *V Mire Nerazrush. Kontr*, (1), 64-70.